Proceedings of the ASME 2019
Dynamic Systems and Control Conference
DSCC2019
October 8-11, 2019, Park City, UT, USA

DSCC2019-9191

NEURAL-NETWORK BASED ITERATIVE LEARNING CONTROL OF A HYBRID EXOSKELETON WITH AN MPC ALLOCATION STRATEGY

Vahidreza Molazadeh[1], Qiang Zhang[1], Xuefeng Bao[1], Nitin Sharma[1, 2 *]
[1]The Department of Mechanical Engineering and Materials Science, University of Pittsburgh
[2]The Department of Bioengineering, University of Pittsburgh
Pittsburgh, PA

ABSTRACT

In this paper, a novel neural network based iterative learning controller for a hybrid exoskeleton is presented. The control allocation between functional electrical stimulation and knee electric motors uses a model predictive control strategy. Further to address modeling uncertainties, the controller identifies the system dynamics and input gain matrix with neural networks in an iterative fashion. Virtual constraints are employed so that the system can use a time invariant manifold to determine desired joint angles. Simulation results show that the controller stabilizes the hybrid system for sitting to standing and standing to sitting scenarios.

Keywords: Iterative learning controller, Functional electrical stimulation, Model predictive control, Neural network, Virtual constraints

1. INTRODUCTION

A hybrid exoskeleton (HES) is a potential rehabilitation technology that can be used to restore a person's lost walking ability. It provides benefits of both functional electrical stimulation (FES) and a powered exoskeleton. For example additional therapeutic benefits of FES such as muscle growth and increased bone density can be gained through the use of an HES. Additionally, the size and weight of bulky motors and batteries that are deployed in sole powered exoskeletons can be reduced [1]. The powered exoskeleton can also be used to compensate for the effects of FES-induced muscle fatigue. However controlling this type of devices faces several challenges. Firstly, to control the HES, an allocation strategy is needed to coordinate FES and the powered exoskeleton based on the onset of FES-induced muscle fatigue. Our previous paper [2] extended a fatigue based switching control design in [3] for allocating FES and exoskeleton a multi degrees of freedom (DOF) walking. In an alternative approach, inspiration from the muscle synergy principle was used in [4] to address the FES and exoskeleton allocation problem. The method uses a low dimensional controller which controls multiple effectors: FES of multiple muscles and electric motors.

Nonlinearity and uncertainty in the dynamic model of HES are another set of challenges that may impede its day-to-day implementation in a clinical setting. Nonlinear robust control methods like robust integral of the sign of the error [5] and sliding mode control [6] have been designed and analyzed for robust FES control. However these methods rely on high control gains or high frequency to compensate for modeling uncertainties. [7] uses a robust Lyapunov-based MPC that incorporates a contractive constraint. It achieves the system stability despite unknown constants for muscle activation however it suffers from high control gains. Iterative learning control (ILC) [2] and neural-network (NN) based controllers [8] are the approaches that can be utilized to overcome the drawbacks of traditional controller methods, especially for achieving a desired transient response when the system of interest has a repetitive operation. In [8], for controlling neuromuscular electrical stimulation, an NN based controller was proposed. However none of these methods were designed for an HES. Even in our previous work on HES control [2], the controller used feedback linearization and a second-order sliding mode control for both FES and electric motors, but the controller still needed a nominal model for feedback linearization.

In this paper, for addressing the actuation coordination and redundancy problems, a model predictive control (MPC) strategy for optimal allocation of control inputs from motor and FES is used. A virtual constraint [9] that generates desired movements for joints based on a time-invariant manifold is used. For overcoming the problem of uncertain HES dynamics, a novel

* Contact author: nis62@pitt.edu

NN based ILC method is used so that the controller can learn the HES dynamics during its operation. This method addresses the limitation in our previous research in [2] where exact model knowledge (EMK) is required for implementing that controller. In our another previous work [10] a sole ILC method was used to learn a linearly parameterizable part of the system dynamics. Therefore, in this paper a unified (virtual constraint + robust NN based ILC + MPC based allocation) is designed to estimate both linearly parameterizable and non-parameterizable parts of the system dynamics of a generalized HES. The controller tracking stability is proven using an energy based method. Simulations are done for standing to sitting and siting to standing scenarios using this control method.

2. GENERAL HYBRID EXOSKELETON DYNAMIC MODEL

An *N*-DOF hybrid exoskeleton generalized dynamic model can be represented as

$$\dot{x} = f(x) + g_F(x)u_F + g_M(x)u_M \tag{1}$$

where $x = \left[\theta, \dot{\theta}\right]^T, \theta \in \mathbb{R}^N$ is represented as $\theta = [\theta_1, \theta_2, ..., \theta_N]$. $\theta_i \ (i = 1,2,...,N)$ is the angular position of the i^{th} linkage.

$$f(x) = \begin{bmatrix} \mathrm{O}_{N\times N},\ I_{N\times N} \\ J(q)^{-1}(\tau_p - G(\theta) - C(\dot{\theta},\theta)\dot{\theta}) \end{bmatrix} \tag{2}$$

$$g_F(x) = \begin{bmatrix} \mathrm{O}_{2N\times N} \\ J(\theta)^{-1}(B_F(\theta)) \end{bmatrix} \tag{3}$$

$$g_M(x) = \begin{bmatrix} \mathrm{O}_{N\times N} \\ J(\theta)^{-1}(B_M(\theta)) \end{bmatrix} \tag{4}$$

where $B_F \in \mathbb{R}^{N\times 2N}$ is the control gain matrix of FES and $B_M \in \mathbb{R}^{N\times N}$ is the control gain matrix of motors, respectively. $J(\theta) \in \mathbb{R}^{N\times N}$ is the inertia matrix, $G(\theta) \in \mathbb{R}^N$ is the gravitational vector and $C(\dot{\theta},\theta) \in \mathbb{R}^{N\times N}$ is the Centripetal-Coriolis matrix. $u_F \in \mathbb{R}^{2N}$ is the normalized FES input, $u_M \in \mathbb{R}^N$ is the motors current amplitude and $\tau_p \in \mathbb{R}^N$ is the passive moment of muscles.

3. CONTROL DEVELOPMENT

3.1 Virtual Constraint Design and Optimization

The output of that *N*-DOF HES $y \in \mathbb{R}^N$ can be defined as

$$y = h_0(\theta) - h_d(\rho(\theta)) \tag{5}$$

where $h_0(\theta)$ is an independent joint angles function and $h_d(\rho(\theta))$ is a desired virtual constraint function and using the Bezier polynomials, it can be described as

$$h_d\left(\rho(\theta)\right) = \begin{bmatrix} b_1\left(w(\theta)\right) \\ b_2\left(w(\theta)\right) \\ \vdots \\ b_{N-1}\left(w(\theta)\right) \end{bmatrix} \tag{6}$$

Where

$$b(w) = \sum_{k=0}^{M} \varrho_k \frac{M!}{k!(M-k)!} w^k (1-w)^{M-k} \tag{7}$$

In (7), ϱ_k is the optimization search variable and is chosen optimally by an optimization process for a minimum control effort criteria. *M* is an integer, showing the number of Bezier polynomial terms and *w* is derived using the following equation

$$w(\theta) = \frac{\rho(\theta) - \rho^+}{\rho^- - \rho^+} \tag{8}$$

where $\rho(\theta) = \zeta_1\theta_1 + \zeta_2\theta_2 + ... + \zeta_n\theta_N . \zeta_i \in \mathbb{R}$ is designed in a way that $\rho(\theta)$ is monotonically increasing. Minimum value and maximum value of $\rho(\theta)$ are ρ^- and ρ^+, respectively.

3.2 Controller Design

The output y can be written as $y = h(\theta) = h_0(\theta) - h_d(\rho(\theta))$. Therefore

$$\frac{d^2y}{dt^2} = L_f^2 h(\theta) + L_{g_F} L_f h(\theta) u_F + L_{g_M} L_f h(\theta) u_M \tag{9}$$

where $L_{g_F} L_f h$ and $L_{g_M} L_f h$ are the decoupling matrices. The uniqueness and existence of zero dynamics in the neighborhood of a point is guaranteed by the matrices invertibility at the point [11]. $\overline{y}_{1_i} = y_i, \overline{y}_{2_i} = \dot{y}_i, u_1 = u_{F,i}$ and u are defined where subscription of *i* means i^{th} row of a vector. Therefore, the following equations can be derived

$$\begin{aligned} \dot{\overline{y}}_{1_i} &= \overline{y}_2 \\ \dot{\overline{y}}_{2_i} &= \sigma^T v_{f_1} + v_{f_2} + \Omega u_1 + v_g u_2 + v_d \end{aligned} \tag{10}$$

where $\sigma^T v_{f_1} + v_{f_2}$ is equal to i^{th} row of $L_f^2 h(\theta, \dot{\theta}), v_g$ and Ω are equal to i^{th} row of $L_{g_M} L_f h(\theta)$ and $L_{g_F} L_f h(\theta)$, respectively. $\sigma^T v_{f_1}$ is i^{th} row of the linearly parameterizable (LP) part of $L_f^2 h(\theta, \dot{\theta})$ and v_{f_2} is i^{th} row of the non LP part of $L_f^2 h(\theta, \dot{\theta})$. v_d is the system disturbance term and is bounded by b_d, σ^T and v_{f_2} are unknown functions which will be learned by an iterative learning method, and Ω will be learned by a recurrent NN (RNN) which is trained by back propagation. v_{f_2} and Ω can be described by two NNs as follows

$$v_{f_2} = W^T \Theta(V^T X) + \varepsilon_1\left(X\right) \tag{11}$$

$$\Omega = R^T \phi(X) + \varepsilon_2(X) \tag{12}$$

where both NNs augmented input, $X \in \mathbb{R}^{2N+1}$ is defined as $X = \begin{bmatrix} 1 & x \end{bmatrix}^T$. The dimensions of ideal weight matrices for first NN are $W \in \mathbb{R}^{N_2+1}$ and $V \in \mathbb{R}^{(2N+1)\times N_2}$, and the dimension of ideal weight matrix for the second NN is $R \in \mathbb{R}^{N_\Omega}$. 2*N*+1 neurons compose the input layer. The hidden layers of the NNs are made of $N_2 \in I^+$ and $N_\Omega \in I^+$ neurons. $\Theta : \mathbb{R}^{N_2} \to \mathbb{R}^{N_2+1}$ is the activation function of first NN in (11) and it maps the input layer to the hidden layers. $\phi : \mathbb{R}^{2N+1} \to \mathbb{R}^{N_\Omega}$ is the activation function in (12) and it maps the input layer to the output layer. $\varepsilon_1 \in \mathbb{R}$ and $\varepsilon_2 \in \mathbb{R}$ are the unknown functional reconstruction errors for the two NNs and are bounded as $|\varepsilon_1| \le \bar{\varepsilon}$ _{1} and $|\varepsilon_2| \le \bar{\varepsilon}_2$ where $\bar{\varepsilon}_1, \bar{\varepsilon}_2 \in \mathbb{R}^+$. The ideal NN's, v_{f_2} and Ω can be estimated by $\hat{v}_{f_{2,k}}$ and $\hat{\Omega}_k$, which can be described as

$$\hat{v}_{f_{2,k}} = \hat{W}_k^T \Theta(\hat{V}_k^T X_k) \tag{13}$$

$$\hat{\Omega}_k = \hat{R}_k^T \phi(X_k) \tag{14}$$

where $\hat{W}_k \in \mathbb{R}^{N_2+1}, \hat{V}_k \in \mathbb{R}^{(2N+1)\times N_2}$ and $\hat{R}_k \in \mathbb{R}^{N_\Omega}$ are the estimates of ideal weights in k^{th} iteration. For stabilizing the generalized HES, based on the motor virtual input u_2 and FES virtual input u_1, the following virtual input is defined

$$u_1 = \psi_k^{-1}\left(-\bar{u}_1 - \hat{v}_{f_{2,k}} - \hat{\sigma}_k^T v_{f_1}\right) \tag{15}$$

where ψ_k is represented as

$$\psi_k = \hat{\Omega}_k + \left(\varrho\left(\hat{\Omega}_k\right) + \beta\right). \tag{16}$$

In (15) and (16), $\hat{\Omega}_k$ and $\hat{v}_{f_{2,k}}$ are the estimates of Ω and v_{f_2}, respectively. $\hat{\sigma}_k$ is an estimate for σ. The spectral radius of $\hat{\Omega}$, $\varrho\left(\hat{\Omega}\right) \in \mathbb{R}^+$, and a control gain $\beta \in \mathbb{R}^+$ are added to ψ [12] to avoid the singularity when $\hat{\Omega}$ is equal to zero. $\bar{u}_1 \in \mathbb{R}$ is added as an additional feedback input. Based on the subsequent stability analysis, weight matrices update law are designed as

$$\hat{W}_{k_j} = \hat{W}_{k_{j-1}} - \kappa_1 \frac{\partial E_b}{\partial \hat{W}_{k_{j-1}}} \tag{17}$$

$$\hat{V}_{k_j} = \hat{V}_{k_{j-1}} - \kappa_2 \frac{\partial E_b}{\partial \hat{V}_{k_{j-1}}} \tag{18}$$

where $\kappa_1 \in \mathbb{R}^+$ and $\kappa_2 \in \mathbb{R}^+$ are constants that have direct effect on the convergence speed. E_b is defined as

$$E_b = \frac{1}{2}\left(\hat{v}_{f_{2,k}} - \hat{v}_{f_{2,k-1}} - \xi\gamma s_k\right)^T \left(\hat{v}_{f_{2,k}} - \hat{v}_{f_{2,k-1}} - \xi\gamma s_k\right) \tag{19}$$

The sliding surface $s_k \in \mathbb{R}$ is defined as $s_k = \lambda_1 e_k(t) + \lambda_2 \dot{e}_k(t)$, where $e_k = (\bar{y}_{1_i,d} - \bar{y}_{1_i})$. λ_1 and λ_2 are positive constants, $\bar{y}_{1_i}$ is the actual output of the system, $\bar{y}_{1_i,d}$ is the desired output of the system. $\xi \in \mathbb{R}^+$ and $\gamma \in \mathbb{R}^+$ are positive constants. Additionally, update laws for the ideal weight estimation $\hat{R}_k$ and the system LP part estimation $\hat{\sigma}_k$ are described by the following equations based on the stability analysis in the next section

$$\dot{\hat{R}}_k = -\phi(X_k) u_{1,k} s_k^T \tag{20}$$

$$\hat{\sigma}_k = \hat{\sigma}_{k-1} - b_q v_{f_1}^T(\gamma s_k) \tag{21}$$

where $b_q \in \mathbb{R}^+$ is a positive constant. By subtracting and adding ψ_k and substituting (15) to (10), the following result is obtained

$$\dot{\bar{y}}_{2_i,k} = E_{s,k} + \Psi_k^T v_{f_1} + \tilde{\Omega}_k u_1 - \bar{u}_1 + v_g u_2 + v_d \tag{22}$$

where $E_{s,k} = v_{f_2} - \hat{v}_{f_{2,k}}$, $\tilde{\Omega}_k = \Omega - \psi_k$ and $\Psi_k = \sigma - \hat{\sigma}_k$. $\tilde{\Omega}_k$ can be also represented as the following equation based on (16) and (12)

$$\tilde{\Omega}_k = \tilde{R}_k^T \phi(X_k) + \beta_\varepsilon \tag{23}$$

where $\beta_\varepsilon = \varepsilon_2(X) - \left(\varrho\left(\hat{\Omega}\right) + \beta\right)$ and it is bounded by $\bar{\beta}_\varepsilon \in \mathbb{R}^+$, and $\tilde{R} = R - \hat{R}$. Hence (22) can be written as

$$\dot{\bar{y}}_{2_i,k} = E_{s,k} + \Psi_k^T v_{f_1} + (\tilde{R}_k^T \phi(X_k) + \beta_\varepsilon) u_1 - \bar{u}_1 + v_g u_2 + v_d \tag{24}$$

In the following part, a NN based ILC with MPC allocation stability analysis is provided.

In (24), the following inputs are defined

$$\bar{u}_{1,k} = \frac{\iota_n}{\lambda_2}\left(-\sum_{j=1}^{2} \lambda_j \bar{y}_{j_i,d} + \lambda_1 \bar{y}_{2_i} - \lambda_2\left(\alpha_3 s_k + \frac{4}{3}\alpha_2 sgn(s_k)\right) + \lambda_2 v_k\right) \tag{25}$$

$$u_{2,k} = \varsigma_n v_g^{-1}\left(\left(\alpha_3 s_k + \frac{4}{3}\alpha_2 sgn(s_k) - v_k\right) + \frac{1}{\lambda_2}\left(\sum_{j=1}^{2} \lambda_j \bar{y}_{j_i,d} - \lambda_1 \bar{y}_{2_i}\right)\right) \tag{26}$$

$$\iota_n + \varsigma_n = 1 \tag{27}$$

where $\alpha_2 \in \mathbb{R}, \alpha_3 \in \mathbb{R}^+, \iota_n$ and ς_n are allocation coefficients. v_k is an integrator term that is described as

$$\dot{v}_k = -\beta_1 s_k - \beta_2 v_k \tag{28}$$

where $\beta_1 \in \mathbb{R}^+$ and $\beta_2 \in \mathbb{R}^+$. $\dot{s}_k = \lambda_1 \dot{e}_k(t) + \lambda_2 \ddot{e}_k(t)$ and based on (24)-(27), it can be expanded as

$$\begin{aligned} \dot{s}_k = \lambda_2 \Bigg(& -\alpha_3 s_k - \frac{4}{3}\alpha_2 sgn(s_k) + v_k - v_d \\ & -\Psi_k^T v_{f_1} - \beta_\varepsilon u_{1,k} - \tilde{R}_k^T \phi(X_k) u_{1,k} - E_{s,k} \Bigg) \end{aligned} \tag{29}$$

where ι_n and ς_n are allocated by a MPC allocation strategy.

3.3 Stability Analysis and the Finite Time Convergence

The following energy function is designed for stability analysis of the proposed controller as

$$V_k = V_k^{(1)} + V_k^{(2)} + V_k^{(3)} + V_k^{(4)} + V_k^{(5)} \tag{30}$$

where $V_k^{(1)} = \frac{v_k^T v_k}{2}$, $V_k^{(2)} = \frac{\gamma}{\lambda_2}\frac{s_k^T s_k}{2}$, $V_k^{(3)} = \frac{1}{2b_q}\int_{t_{0,k}}^{t} \Psi_k^T(\tau)\Psi_k(\tau)d\tau$, $V_k^{(4)} = \frac{1}{2\xi}\int_{t_{0,k}}^{t} {E_{s,k}}^T(\tau) E_{s,k}(\tau) d\tau$, and $V_k^{(5)} = \frac{1}{2} tr\left\{\tilde{R}_k^T \tilde{R}_k\right\}$. $t_{0,k}$ is the start time of k^{th} iteration and $\gamma, b_q, \xi \in \mathbb{R}^+$. At the start of each iteration, it is considered that the exoskeleton user starts from the same siting position. Therefore, the difference between first Lyapunov function in two iterations can be expressed as

$$\Delta V_k^{(1)} = V_k^{(1)} - V_{k-1}^{(1)}. \tag{31}$$

$\Delta V_k^{(1)}$ can also be expressed as

$$\Delta V_k^{(1)} = \frac{v_k^T v_k}{2} - \frac{v_{k-1}^T v_{k-1}}{2} = \int_{t_{0,k}}^{t} v_k^T \dot{v}_k d\tau - v_{k-1}^T v_{k-1} \tag{32}$$

By substituting (28) to equation (32), it can be simplified as

$$\Delta V_k^{(1)} = -\beta_1 \int_{t_{0,k}}^{t} v_k^T s_k \, d\tau - \beta_2 \int_{t_{0,k}}^{t} v_k^T v_k \, d\tau - \frac{v_{k-1}^T v_{k-1}}{2}. \tag{33}$$

The difference of the second energy function in two executive iterations is obtained by

$$\Delta V_k^{(2)} = \frac{\gamma}{\lambda_2}\frac{s_k^T s_k}{2} - \frac{\gamma}{\lambda_2}\frac{s_{k-1}^T s_{k-1}}{2} = \frac{\gamma}{\lambda_2}\int_{t_{0,k}}^{t} s_k^T \dot{s}_k d\tau - \frac{\gamma}{\lambda_2}\frac{s_{k-1}^T s_{k-1}}{2} \tag{34}$$

Similarly, (34) can be simplified by substituting (29)

$$\begin{aligned} \Delta V_k^{(2)} = & -\frac{\gamma}{\lambda_2}\frac{s_{k-1}s_{k-1}}{2} \\ & -\gamma \int_{t_{0,k}}^{t} s_k^T \Psi_k^T v_{f_1} d\tau - \frac{4}{3}\alpha_2 \gamma \int_{t_{0,k}}^{t} s_k^T sgn(s_k) d\tau \\ & -\gamma \int_{t_{0,k}}^{t} s_k^T v_d \, d\tau - \gamma \int_{t_{0,k}}^{t} s_k^T \tilde{R}_k^T \phi(X_k) u_{1,k} \, d\tau \\ & -\gamma\alpha_3 \int_{t_{0,k}}^{t} s_k^T s_k \, d\tau - \gamma \int_{t_{0,k}}^{t} s_k^T \beta_\varepsilon u_{1,k} \, d\tau \\ & +\gamma \int_{t_{0,k}}^{t} s_k^T v_k \, d\tau - \gamma \int_{t_{0,k}}^{t} s_k^T E_{s,k} \, d\tau \end{aligned} \tag{35}$$

where b_d and $\bar{\beta}_\varepsilon$ are upper bounds of v_d and β_ε, respectively. Accordingly,

$$\begin{aligned} \Delta V_k^{(2)} \le & -\frac{\gamma}{\lambda_2}\frac{s_{k-1}s_{k-1}}{2} \\ & +b_d \gamma \int_{t_{0,k}}^{t} |s_k| d\tau + \gamma \int_{t_{0,k}}^{t} s_k^T v_k \, d\tau \\ & -\gamma \int_{t_{0,k}}^{t} s_k^T \Psi_k^T v_{f_1} d\tau + \frac{4}{3}\alpha_2 \gamma \int_{t_{0,k}}^{t} |s_k| d\tau \\ & -\gamma \int_{t_{0,k}}^{t} s_k^T E_{s,k} \, d\tau - \gamma \int_{t_{0,k}}^{t} s_k^T \tilde{R}_k^T \phi(X_k) u_{1,k} \, d\tau \\ & -\gamma\alpha_3 \int_{t_{0,k}}^{t} s_k^T s_k \, d\tau + \gamma \int_{t_{0,k}}^{t} |s_k| \bar{\beta}_\varepsilon \, d\tau \end{aligned} \tag{36}$$

The difference of the third energy function can be written as

$$\Delta V_k^{(3)} = \frac{1}{2b_q}\int_{t_{0,k}}^{k} \Psi_k^T \Psi_k d\tau - \frac{1}{2b_q}\int_{t_{0,k}}^{k} \Psi_{k-1}^T \Psi_{k-1} d\tau \tag{37}$$

where the following equation can be derived based on [13]

$$\begin{aligned} & \frac{1}{2b_q}\left(\Psi_k^T \Psi_k - \Psi_{k-1}^T \Psi_{k-1}\right) \\ & = \frac{1}{2b_q}\left(\hat{\sigma}_k - \hat{\sigma}_{k-1}\right)^T \left(\hat{\sigma}_k + \hat{\sigma}_{k-1} - 2\sigma\right)^T \\ & = \frac{1}{b_q}\left(\hat{\sigma}_k - \sigma\right)^T \left(\hat{\sigma}_k - \hat{\sigma}_{k-1}\right) \\ & -\frac{1}{2b_q}\left(\hat{\sigma}_k - \hat{\sigma}_{k-1}\right)^T \left(\hat{\sigma}_k - \hat{\sigma}_{k-1}\right) \end{aligned} \tag{38}$$

Considering (21), (38) can be written as

$$\frac{1}{2b_q}\left(\Psi_k^T\Psi_k-\Psi_{k-1}^T\Psi_{k-1}\right)==$$
$$\gamma\Psi_k^T s_k^T v_{f_1}$$
$$-\frac{1}{2b_q}\left(\hat{\sigma}_k-\hat{\sigma}_{k-1}\right)^T\left(\hat{\sigma}_k-\hat{\sigma}_{k-1}\right) \quad . \tag{39}$$

Therefore, (37) is obtained as

$$\Delta V_k^{(3)}=-\frac{1}{2b_q}\int_{t_{0,k}}^{t}\left(\hat{\sigma}_k-\hat{\sigma}_{k-1}\right)^T\left(\hat{\sigma}_k-\hat{\sigma}_{k-1}\right)d\tau$$
$$+\gamma\int_{t_{0,k}}^{t}\left(\Psi_k^T s_k^T v_{f_1}\right)d\tau \quad . \tag{40}$$

The fourth energy function difference between two executive iterations is

$$\Delta V_k^{(4)}=\frac{1}{2\xi}\int_{t_{0,k}}^{k}E_{s,k}{}^T E_{s,k}\,d\tau-\frac{1}{2\xi}\int_{t_{0,k}}^{k}E_{s,k-1}{}^T E_{s,k-1}\,d\tau. \tag{41}$$

The following equation can be written similar to the previous energy function

$$\frac{1}{2\xi}\left(E_{s,k}{}^T E_{s,k}-E_{s,k-1}{}^T E_{s,k-1}\right)=\frac{1}{\xi}E_{s,k}^T\left(\hat{v}_{f_{2,k}}-\hat{v}_{f_{2,k-1}}\right)$$
$$-\frac{1}{2\xi}\left(\hat{v}_{f_{2,k}}-\hat{v}_{f_{2,k-1}}\right)^T\left(\hat{v}_{f_{2,k}}-\hat{v}_{f_{2,k-1}}\right) \tag{42}$$

By substituting (19), it is concluded that

$$\Delta V_k^{(4)}=\gamma E_{s,k}^T s_k-\frac{1}{2\xi}\left(\hat{v}_{f_{2,k}}-\hat{v}_{f_{2,k-1}}\right)^T\left(\hat{v}_{f_{2,k}}-\hat{v}_{f_{2,k-1}}\right) \tag{43}$$

Hence

$$\Delta V_k^{(4)}=-\frac{1}{2\xi}\int_{t_{0,k}}^{t}\left(\hat{v}_{f_{2,k}}-\hat{v}_{f_{2,k-1}}\right)^T\left(\hat{v}_{f_{2,k}}-\hat{v}_{f_{2,k-1}}\right)d\tau$$
$$+\gamma\int_{t_{0,k}}^{t}\left(s_k^T E_{s,k}\right)d\tau \quad . \tag{44}$$

The fifth energy function difference is

$$\Delta V_k^{(5)}=\frac{1}{2}tr\left\{\tilde{R}_k^T\tilde{R}_k\right\}-\frac{1}{2}tr\left\{\tilde{R}_{k-1}^T\tilde{R}_{k-1}\right\} \tag{45}$$

which can be rearranged as

$$\Delta V_k^{(5)}=-tr\left\{\int_{t_{0,k}}^{t}\tilde{R}_k^T\dot{\tilde{R}}_k\,d\tau\,d\tau\right\}-\frac{1}{2}tr\left\{\tilde{R}_{k-1}^T\tilde{R}_{k-1}\right\}. \tag{46}$$

By substituting (20) in (46), $\Delta V_k^{(5)}$ can be expanded as

$$\Delta V_k^{(5)}=-\frac{1}{2}tr\left\{\tilde{R}_{k-1}^T\tilde{R}_{k-1}\right\}$$
$$-tr\left\{\int_{t_{0,k}}^{t}\tilde{R}_k^T\left(-\phi\left(X_k\right)u_{1,k}s_k^T\right)d\tau\right\} \quad . \tag{47}$$

By summing the difference of five energy terms between two executive iterations and considering $\beta_1=\gamma$ and $\alpha_2=\frac{-3(b_d+\bar{\beta}_\varepsilon)}{4}$, the following ultimate inequality is obtained as

$$\Delta V_k=\Delta V_k^1+\Delta V_k^2+\Delta V_k^3+\Delta V_k^4+\Delta V_k^5$$
$$\le-\frac{v_{k-1}^T v_{k-1}}{2}-\frac{\gamma}{\lambda_2}\frac{s_{k-1}^T s_{k-1}}{2}-\gamma\alpha_3\int_{t_{0,k}}^{t}s_k^T s_k\,d\tau$$
$$-\frac{1}{2\xi}\int_{t_{0,k}}^{t}\left(\hat{v}_{f_{2,k}}-\hat{v}_{f_{2,k-1}}\right)^T\left(\hat{v}_{f_{2,k}}-\hat{v}_{f_{2,k-1}}\right)d\tau \quad . \tag{48}$$
$$-\frac{1}{2b_q}\int_{t_{0,k}}^{t}\left(\hat{\sigma}_k-\hat{\sigma}_{k-1}\right)^T\left(\hat{\sigma}_k-\hat{\sigma}_{k-1}\right)d\tau$$
$$-\frac{1}{2}tr\left\{\tilde{R}_{k-1}^T\tilde{R}_{k-1}\right\}-\beta_2\int_{t_{0,k}}^{t}v_k^T v_k\,d\tau$$

Therefore, $-\Delta V_k$ is a class K function, hence V_k will be decreased. Additionally, because $V_k(t)\in\mathbb{R}^+$, this ensures V_k converges to zero. Accordingly, it can be concluded that the sliding surface and Ψ which shows the estimation error of PL part of the system will go to zero. Also, the errors of both NNs, $E_{s,k}$ and $\tilde{R}_k^T$ will also go to zero. Accordingly, the designed controller in (10) is asymptotically stable. The sliding surface dynamics is Hurwitz, hence, after the convergence of $V_k(t)$, the error of output converges to zero exponentially.

3.4 Model-based Predictive Allocation Strategy

In this part, ι_n and ς_n are allocated by an MPC allocation strategy. The objective index of MPC allocation is designed as

$$\min_{\iota_n(t)}J_a(t_k)=\int_{t_k}^{t_k+T_h}\left(\hat{\tau}_m^2+\frac{w}{\hat{\mu}+\acute{\mathrm{U}}}\hat{\tau}_s^2\right)dt$$
$$\text{s.t. }\iota_n+\varsigma_n=1,\hat{\tau}_m=v_g\hat{u}_2 \tag{49}$$
$$\hat{\tau}_s=\Phi_a\left(\hat{\theta},\dot{\hat{\theta}},\hat{\mu},\hat{u}_1\right),0=\Phi_\mu\left(\dot{\bar{\mu}},\bar{\mu},\hat{u}_1\right)$$

where the terms with a hat, e.g. $\hat{u}_2$, show the nominal variables, which are evaluated in the prediction horizon. $\Phi_a\left(\dot{\hat{\mu}},\hat{\mu},\hat{u}_1\right):\mathbb{R}\times[0,1]\times[0,1]\mapsto\mathbb{R}$ is the differential equation that represents the FES-driven knee torque $\hat{\tau}_s$ based on the stimulation input and the fatigue variable, $\hat{\tau}_m$ is the motor torque input, $\hat{\mu}$, and $\Phi_\mu\left(\dot{\mu},\mu,u_1\right)=0$ is a differential equation that specify fatigue level. $\varepsilon\in\mathbb{R}^+$ and $w\in\mathbb{R}^+$ are positive constants. The FES control allocation $\iota_n(t)$ is the search variable along the time horizon $[t_k,t_k+T_h]$ and has direct effect on objective index

$J_a(t)$. T_h is the length of the prediction horizon and t_k is the current time instant in k^{th} iteration. Initially, suppose $u_1^*\left(t \middle| :t \in \left[t_k, t_k + T_h\right]\right) = \text{argmin}\{J_a(t)\}$ is found, and then $u_1 = u_1^*\left(t \middle| :t = t_k \to t_k + \varepsilon\right)$ is considered for the next iteration, where ε is the time step that makes $t_{k+1} = t_k + \varepsilon$ [14]. The model predictive algorithm is detailed in Table 1.

TABLE 1. DETAILS OF MODEL PREDICTIVE CONTROL ALLOCATION STRATEGY

1	**Initialization:** j=0
(1a)	The tolerance of convergence is set to ε_c .
(1b)	$\theta(t_k), \dot{\theta}(t_k)$ are measured.
(1c)	Virtual constraint and feedback controller are used to get $\mathbf{h}_d(t), \hat{h}(t),$ and $T_1(t)$, where $t \in [t_k, t_k + T_N]$.
(1d)	$\hat{u}_1(t) \in \mathcal{U}_{[t_k, t_k+T_N]}$ is chosen as the initial optimal control guess, where $t \in [t_k, t_k + T_N]$.
(1e)	$\hat{\tau}_s(t)$ and $J_a^{(j)}(t_k)$ are obtained using $\hat{u}_1(t)$ and $\hat{h}(t)$ where $t \in [t_k, t_k + T_N]$.
2	**Searching for an Optimal Solution:**
(2a)	The costate, $l^{(j)}(t)$ is solved using an integration backward in time, H is defined as $H = J_a + l^T \Phi_\mu$, hence an optimal solution is obtained as $\dot{l}(\tau) = -\frac{\partial H(x, l, \hat{u}_1)}{\partial \hat{x}}$, where $\hat{x} = \left[x, \hat{\mu}\right]$.
(2b)	Using the Hamiltonian, the search direction $a^{(j)}(t)$ is obtained as $a^{(j)}(t) = -\frac{\partial H(x, l, \hat{u}_1)}{\partial \hat{u}_1}$.
(2c)	By using the adaptive setting in [15], the optimal step size, $\sigma^{(j)}$ is computed.
(2d)	The control is updated. $\hat{u}_1^{(j+1)}(t) = \zeta(\hat{u}_1^{(j)} + \sigma^{(j)} a^{(j)})$, where ζ represents the constraints.
(2e)	$\hat{u}_1^{(j+1)}$ is utilized to get $J_a^{(j+1)}(t_k)$.
(2f)	Quit conditions are checked (i) if $\left\|J_a^{(j+1)}(t_k) - J_a^{(j)}(t_k)\right\| \le \varepsilon_c$ is satisfied, quit. (ii) if j exceeds the max iteration number N_t , quit. (iii) otherwise j=j+1 and from (1a) reiterate gradient step.

4. SIMULATION RESULTS

After implementing the controller on the system for siting to standing and standing to sitting scenarios, the MPC algorithm allocates the knee FES torque according to the Fig. 1. This allocation causes a normalized fatigue trend which is shown in the Fig. 2.

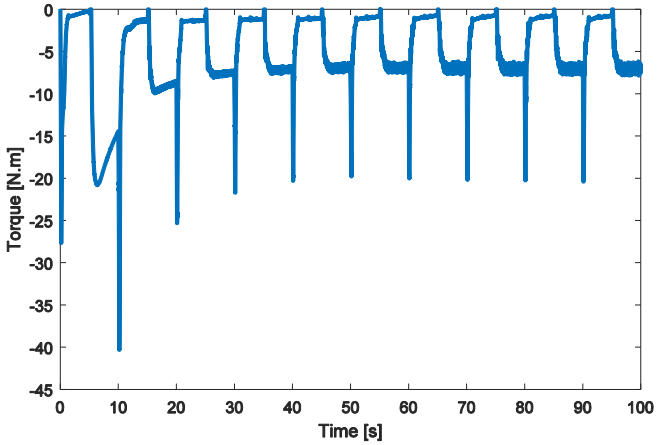

FIGURE 1: FES TORQUE ALLOCATION ON THE KNEE JOINT BY USING MPC

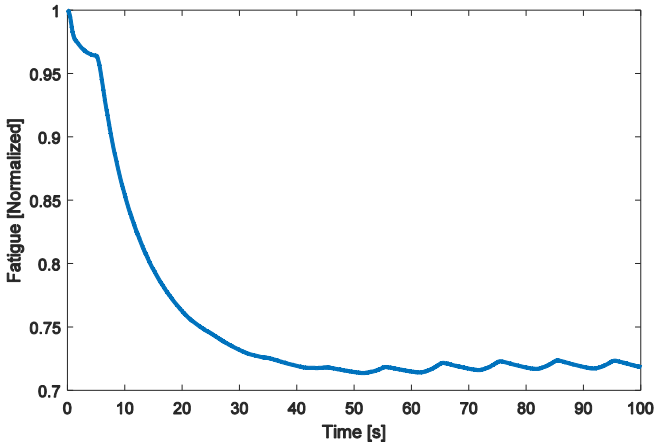

FIGURE 2: NORMALIZED FATIGUE OVER TIME

The desired and actual trajectories of hip and knee joints are demonstrated in Fig. 3. In this figure, θ_1 is the knee joint angle and θ_2 is the hip joint angle.

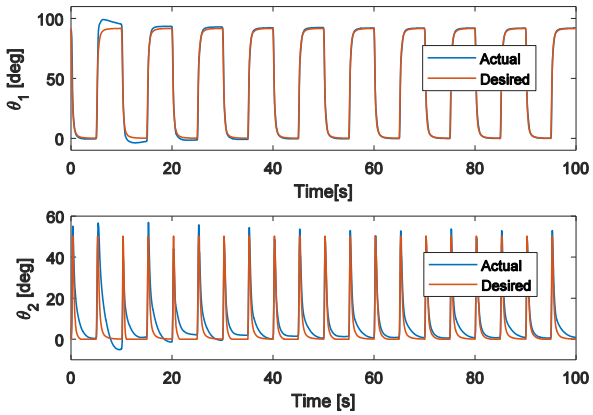

FIGURE 3: JOINT ANGLES OVER TIME

According to Fig. 4, compared to the first iteration, the 10^{th} iteration of the algorithm could reduce 86% of root mean square (RMS) error of the knee joint angle tracking performance and 57% of RMS error of the hip joint angle tracking performance.

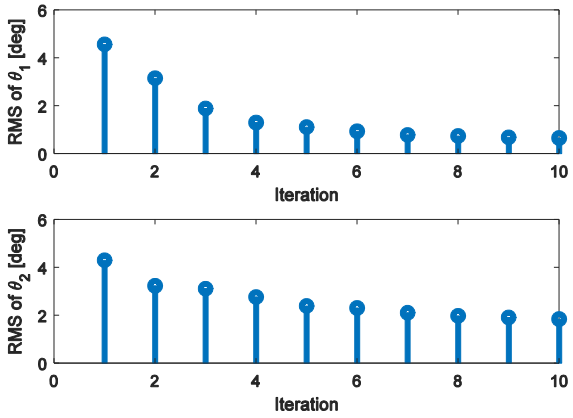

FIGURE 4: ROOT MEAN SQUARE OF THE JOINT ANGLES ERROR VS ITERATIONS

5. CONCLUSION

A cooperative control strategy for a hybrid exoskeleton was designed. An MPC allocation was used to optimally allocate FES and knee motor torques based on the muscle fatigue dynamics. Its ability to balance the stimulation and robotic actuation was shown in siting to standing and standing to sitting scenarios. The NN based ILC makes the system robust to system uncertainties and day-to-day parametric variations. The results show decline in the system RMS error after each iteration for the targeted scenario. Thus the simulations showed the effectiveness of the controller to improve the tracking performance.

ACKNOWLEDGEMENTS

Research reported in this article is supported in part by Eunice Kennedy Shriver National Institute of Child Health and Human Development of the National Institutes of Health under award number: R03HD086529. The content is solely the responsibility of the author(s) and does not necessarily represent the official views of the National Institutes of Health. The national science foundation (NSF) also funded this work in part by the award number: 1511139. Any recommendations, opinions, conclusions and findings expressed in this material are those of the author(s) and do not necessarily reflect the National Science Foundation views.

REFERENCES

[1] N. A. Alibeji, V. Molazadeh, B. E. Dicianno, and N. Sharma, "A Control Scheme That Uses Dynamic Postural Synergies to Coordinate a Hybrid Walking Neuroprosthesis: Theory and Experiments," *Front. Neurosci.*, vol. 12, p. 159, Apr. 2018.

[2] V. Molazadeh, Z. Sheng, and N. Sharma, "A Within-Stride Switching Controller for Walking with Virtual Constraints: Application to a Hybrid Neuroprosthesis," in *2018 Annual American Control Conference (ACC)*, 2018, pp. 5286–5291.

[3] N. Kirsch, N. Alibeji, B. E. Dicianno, and N. Sharma, "Switching control of functional electrical stimulation and motor assist for muscle fatigue compensation," in *2016 American Control Conference (ACC)*, 2016, pp. 4865–4870.

[4] N. A. Alibeji, V. Molazadeh, F. Moore-Clingenpeel, and N. Sharma, "A Muscle Synergy-Inspired Control Design to Coordinate Functional Electrical Stimulation and a Powered Exoskeleton: Artificial Generation of Synergies to Reduce Input Dimensionality," *IEEE Control Syst.*, vol. 38, no. 6, pp. 35–60, Dec. 2018.

[5] N. Sharma, K. Stegath, C. M. Gregory, and W. E. Dixon, "Nonlinear Neuromuscular Electrical Stimulation Tracking Control of a Human Limb," *IEEE Trans. Neural Syst. Rehabil. Eng.*, vol. 17, no. 6, pp. 576–584, Dec. 2009.

[6] R. Bkekri, A. Benamor, M. A. Alouane, G. Fried, and H. Messaoud, "Robust adaptive sliding mode control for a human-driven knee joint orthosis," *Ind. Robot An Int. J.*, vol. 45, no. 3, pp. 379–389, May 2018.

[7] Z. Sun, X. Bao, and N. Sharma, "Lyapunov-based Model Predictive Control of an Input Delayed Functional Electrical Simulation," *IFAC-PapersOnLine*, vol. 51, no. 34, pp. 290–295, Jan. 2019.

[8] M. J. Khodaei, M. H. Balaghi I., A. Mehrvarz, and N. Jalili, "An Adaptive Multi-critic Neuro-fuzzy Control Framework for Intravenous Anesthesia Administration," *IFAC-PapersOnLine*, vol. 51, no. 34, pp. 202–207, Jan. 2019.

[9] R. D. Gregg and J. W. Sensinger, "Towards Biomimetic Virtual Constraint Control of a Powered Prosthetic Leg," *IEEE Trans. Control Syst. Technol.*, vol. 22, no. 1, pp. 246–254, Jan. 2014.

[10] V. Molazadeh, Z. Sheng, X. Bao, and N. Sharma, "A Robust Iterative Learning Switching Controller for following Virtual Constraints: Application to a Hybrid Neuroprosthesis," *IFAC-PapersOnLine*, vol. 51, no. 34, pp. 28–33, Jan. 2019.

[11] A. Isidori, *Nonlinear Control Systems*, Springer Science & Business Media, 2013.

[12] M. Chen, S. S. Ge, and B. How, "Robust Adaptive Neural Network Control for a Class of Uncertain MIMO Nonlinear Systems With Input Nonlinearities," *IEEE Trans. Neural Networks*, vol. 21, no. 5, pp. 796–812, May 2010.

[13] W. Chen, Y.-Q. Chen, and C.-P. Yeh, "Robust iterative learning control via continuous sliding-mode technique with validation on an SRV02 rotary plant," *Mechatronics*, vol. 22, no. 5, pp. 588–593, Aug. 2012.

[14] K. Graichen and A. Kugi, "Stability and Incremental Improvement of Suboptimal MPC Without Terminal Constraints," *IEEE Trans. Automat. Contr.*, vol. 55, no. 11, pp. 2576–2580, Nov. 2010.

[15] K. Graichen, B. K.-F, *A real-time gradient method for nonlinear model predictive control*. INTECH Open Access Publisher, 2012.